Dual Energy CT Protocol Optimization for Increased Blood Detectability of Virtual Non-Contrast Images in a Single Source System: A Phantom Study

Catherine Olguin MS*, Izabella Barreto Ph.D., Stephanie Leon Ph.D., Reordan De Jesus M.D., Manuel Arreola Ph.D.
Department of Radiology, College of Medicine , University of Florida

Introduction

Dual-energy CT (DECT) imaging has proven to be useful in the stroke setting, capable of differentiating residual iodinated contrast and hemorrhagic blood. Iodine maps enhance iodine and suppress blood. Virtual non-contrast images suppress iodine and enhance blood products. However, from our experience, blood may be misidentified (or not detected) by DECT, particularly when microhemorrhage is involved.

Purpose: To optimize the DECT stroke protocol in order to improve detectability of hemorrhages in stroke patients, including those with microhemorrhaging. DECT protocols are sensitive to the effective energy of the spectra utilized. Since the vendor-recommended DECT protocols were the same for two CT scanners with different filtration, we sought to identify optimal settings specific to head imaging and the specific scanner used.

Methods

A Gammex multi-energy CT phantom (Model 1472) with stroke-mimicking materials was scanned in a single source sequential DECT scanner (Canon Aquilion ONE Genesis) with the clinical DECT head protocol ($CTDI_{vol}$ =54 mGy). Iodine maps and VNC images were post-processed with the vendor-recommended and optimized stroke protocols. To create the optimized iodine maps and VNCs, the input of two virtual monochromatic images (VMI) with equivalent 135-kVp and 80-kVp soft tissue Hounsfield Units (HU) was required. These were identified as follows:

1. VMIs were reconstructed over a range of 35-135 keV.
2. By least squares optimization (LSO), soft-tissue-equivalent VMIs were identified (Equation 1, Table 1).
3. The iodine contrast slope was measured for the optimized VMIs.
4. Adipose tissue and grey matter HUs were measured in the VMIs.
5. Pixel values from the high- and low-energy data sets were plotted for both the vendor-recommend and optimized soft tissue/fat line.

Next, a comparison of the vendor-recommended and optimized protocol was performed:

1. Iodine and VNC images were reconstructed with the vendor-recommended and the optimized settings.
2. The enhancement of inserts mimicking iodine, acute and chronic blood was measured in iodine maps and VNCs.
3. Contrast-to-noise ratios were calculated for the iodine map and VNC images created from vendor-recommended and optimized settings (Equation 2) for several different background materials (grey, white matter, blood, and iodine).

Table 1. Materials mimicking tissues in stroke imaging used in the LSO equation.

Solid Water
Blood (40,70)
Adipose
Grey Matter
White Matter

$$\text{LSO} = \sum(\text{CT Number}_{\text{VMI}} - \text{CT Number}_{\text{SECT}})^2 \qquad \textbf{Equation 1}$$

$$\text{CNR} = \frac{\text{ROI}_{\text{material}} - \text{ROI}_{\text{background}}}{\sigma_{\text{background}}} \qquad \textbf{Equation 2}$$

Results

Phantom Measurements:

- The optimized VMIs were identified as 71 keV and 57 keV, whereas the vendor-recommended VMIs were 66 keV and 52 keV. The optimized VMI contrast slope changed from 0.55 to 0.59 (Table 2).
- Pixel values from the high- and low-energy data sets were plotted for the vendor-recommend (dashed) and optimized (solid) fat-soft tissue line and contrast slope. Yellow labels indicate the optimized coordinates for the two materials of the fat-grey matter line (Figure 1). Note, the second material of the three-material decomposition algorithm was changed from soft tissue to gray matter. With the selection of grey matter, Blood 40-HU falls above the fat-soft tissue line coordinates rather than within the coordinates. The selection of gray matter may improve the identification, or detection, of Blood 40-HU.
- Iodine enhancement on the optimized-iodine map decreased on average by 20 HU, but iodine 0.2 mg I/mL remained detectable (7.84 HU). While the Blood 70 (acute blood) and Blood 40 (chronic blood) inserts were enhanced in the vendor-iodine map (15 and 5 HU, respectively), neither blood insert enhanced with the optimized-iodine map (0 HU) (Figure 2A).
- Acute and chronic blood HU increased in the optimized-VNC by 2.94 and 11.71 HU, respectively. Iodine HUs increased for concentrations below 2 mg I/mL, but remained below and well-differentiated from Blood-40 (Δ29 HU), grey matter (Δ17 HU), and white matter (Δ18 HU) (Figure 2B) for all iodine concentrations.
- Compared to vendor-iodine maps, optimized-iodine map CNR increased for iodine relative to grey matter, white matter and Blood-40. Since Blood-70 was suppressed to 0 HU (σ=0), the CNR was undefined (Figure 3A).
- Optimized-VNC CNRs between blood and white matter decreased, but increased for blood and grey matter (Figure 3B). Optimized-VNC blood with respect to iodine CNRs decreased with the exception of 5 mg I/mL.

Clinical Case:

- In one clinical case read by a neuroradiologist (Figure 4), microhemorrhaging was detected in the SWI MRI and enhanced more in the optimized-VNC than in the vendor-VNC. An image quality assessment with the neuroradiologist was performed for this clinical case. In comparison to the vendor-VNC, the optimized-VNC had greater contrast, improved gyri delineation and improved differentiation between grey and white matter. However, according to the neuroradiologist, one limitation was noise amplification in the optimized-VNC.

Table 2. Three-material decomposition algorithm vendor-recommended and optimized-LSO settings for DECT stroke imaging.

High- and Low-kV Spectra	Protocol	High- /Low-VMI (keV)	Material 1 Material 2 Material 3	Material 1 and 2 High- and Low-VMI CT Numbers (HU)	Material 3 Iodine Slope
135-kV 80-kV	Vendor-Recommended	66/52 keV	Fat Soft Tissue Iodine	-106/-136 63/67	0.55
	Optimized-LSO	71/57 keV	General Adipose Grey Matter Iodine	-61/-82 30/41	0.59

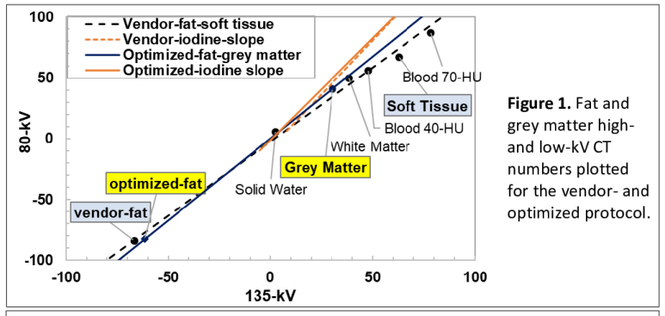

Figure 1. Fat and grey matter high- and low-kV CT numbers plotted for the vendor- and optimized protocol.

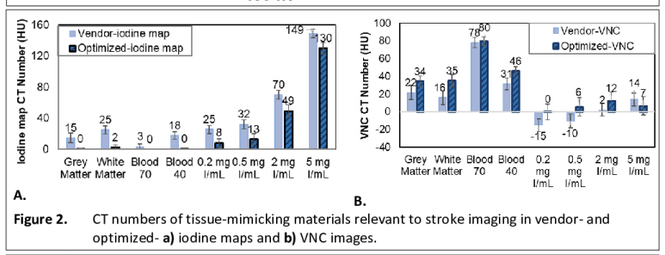

Figure 2. CT numbers of tissue-mimicking materials relevant to stroke imaging in vendor- and optimized- **a)** iodine maps and **b)** VNC images.

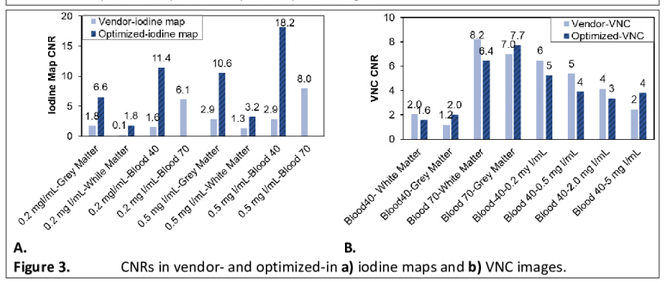

Figure 3. CNRs in vendor- and optimized-in **a)** iodine maps and **b)** VNC images.

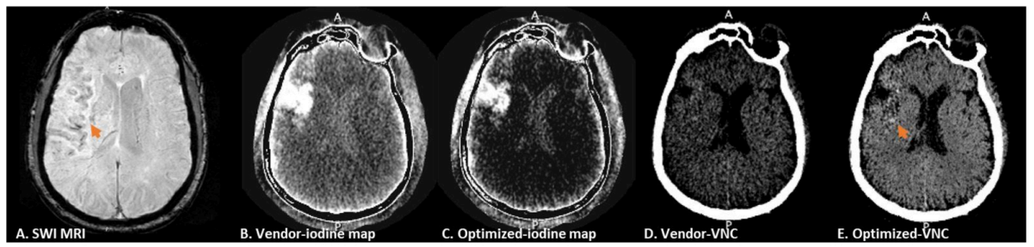

Figure 4. Clinical case where **a)** SWI MRI indicates microhemorrhaging by orange arrow. Both **b-c)** iodine maps show iodine enhancement. However, the **d)** vendor-VNC has light enhancement which was not classified as microhemorrhaging during interpretation. The **e)** optimized-VNC shows enhancement by orange arrow due to microhemorrhagic content as dictated by a neuroradiologist.

Conclusions

DECT vendor-recommended stroke protocols may need optimization for specific clinical tasks such as for microhemorrhage detection. This phantom study optimized the stroke protocol and increased blood enhancement in the VNC in the phantom measurements and clinical case.

Impact: Imaging of microhemorrhaging has been an incidental finding, where only 50% of microbleeds are diagnosed with optimized SWI MRI imaging due to the small 5-10-mm lesion size and iron composition[1]. Microhemorrhaging has been found to contribute to greater long-term disability in comparison to other clinical findings in patients with nonaccidental trauma[2]. Cerebral microhemorrhages are also recognized to have diagnostic and prognostic implications[3]. Therefore, early onset detection of microhemorrhage may aid in proper care of patients, which may improve the patient's overall neurologic outcome.

Limitations: The enhancement shown in the new VNC clinical case may be an effect of increased enhancement of pixels surrounding the iodinated contrast region. Future work will analyze a greater patient sample size to identify the sensitivity, specificity and false positive rate of the new optimized VNC in comparison to SWI MRI.

Acknowledgements and Disclosure

- Dr. Tara Massini, Dr. John Rees, Lori Gravelle, Dr. Amar Dhanantwari, Dr. Erin Angel, Kolo Pelesikoti
- Research funded by Canon Medical Systems USA, Inc.

References

1. Haller S, et al. Cerebral Microbleeds: Imaging and Clinical Significance, Radiology: Volume 287: number 1- April 2018.
2. Colbert C, et al. Value of Cerebral Microhemorrhages Detected with Susceptibility-weighted MR Imaging for Prediction of Long-term Outcome in Children with Nonaccidental Trauma. Radiology. Vol 256. No. 3 Sept 2010.
3. Blitstein MK, Tung GA. MRI of cerebral microhemorrhages. AJR AM J Roentgenol 2007; 189(3):720-725.

Catherine Olguin, Phone: 352-792-4826, Email: ccarranza1@ufl.edu, Web: xray.ufl.edu